iScience

CellPress
OPEN ACCESS

Article

Specific motifs mediate post-synaptic and surface transport of G protein-coupled receptors

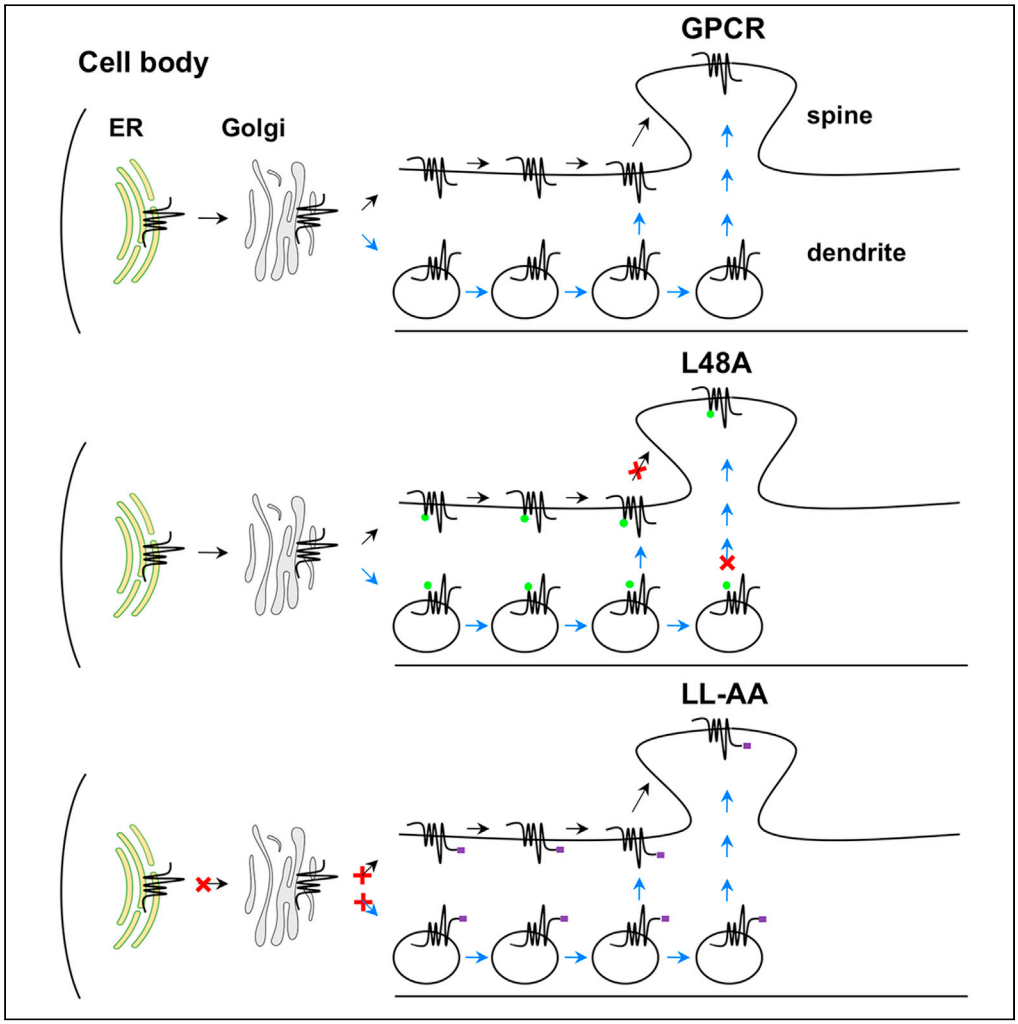

Xin Xu, Zhe Wei, Guangyu Wu

guwu@augusta.edu

Highlights

Leu48 specifically mediates α_{2B}-AR transport to post-synapses in primary neurons

The YS motif differently regulates α_2-AR traffic in neuronal and non-neuronal cells

The LL motif functions as a common export signal for GPCRs in neurons and cell lines

The LL motif confers its transport ability to non-GPCR plasma membrane proteins

Xu et al., iScience *25*, 103643
January 21, 2022
https://doi.org/10.1016/j.isci.2021.103643

iScience

CellPress
OPEN ACCESS

Article

Specific motifs mediate post-synaptic and surface transport of G protein-coupled receptors

Xin Xu,[1,2] Zhe Wei,[1,2] and Guangyu Wu[1,3,*]

SUMMARY

G protein-coupled receptors (GPCRs) are key regulators of synaptic functions. However, their targeted trafficking to synapses after synthesis is poorly understood. Here, we demonstrate that multiple motifs mediate α_{2B}-adrenergic receptor transport to the dendritic and post-synaptic compartments in primary hippocampal neurons, with a single leucine residue on the first intracellular loop being specifically involved in synaptic targeting. The N-terminally located tyrosine-serine motif operates differently in neuronal and non-neuronal cells. We further show that the highly conserved dileucine (LL) motif in the C-terminus is required for the dendritic and post-synaptic traffic of all GPCRs studied. The LL motif also directs the export from the endoplasmic reticulum of a chimeric GPCR and confers its transport ability to vesicular stomatitis virus glycoprotein in cell lines. Collectively, these data reveal the intrinsic structural determinants for the synaptic targeting of nascent GPCRs and their cell-type-specific trafficking along the biosynthetic pathways.

INTRODUCTION

G protein-coupled receptors (GPCRs) modulate a variety of physiological and pathological functions of the nervous system and are direct primary therapeutic targets of numerous neurological disorders (Betke et al., 2012; Chen et al., 2014; Gainetdinov et al., 2004; Roth, 2019; Weinberg et al., 2019). These receptors share many primary amino acid sequences and a common molecular topology characterized by a hydrophobic core of seven membrane-spanning α-helices, and some receptors may form an amphipathic α-helix (also known as helix 8) in the membrane-proximal region of the C-terminus (CT). Whereas the N-terminus (NT), extracellular loops, and transmembrane domains provide the sites responsible for ligand binding, intracellular domains are involved in the regulation of receptor coupling to downstream molecules, signaling initiation, propagation and termination, and trafficking (Pierce et al., 2002; Wang et al., 2004; Wess, 1997; Wu et al., 1997, 1998).

Neurons are specialized cells with unique morphology and compartmentalization. The functions of GPCRs in neurons are under tight control by their trafficking that determines the quality and quantity of the receptors at the synaptic membrane terminals where they are available to bind respective neurotransmitters and activate cognate G proteins or other signaling molecules that in turn activate downstream effectors, including ion channels. In particular, endocytosis that removes the receptors from synapses after agonist activation and anterograde transport that delivers the newly synthesized receptors to synapses are two important but opposing processes that provide important means to regulate neuronal function (Doly et al., 2016; Dong et al., 2007; Lyssand et al., 2010; Retamal et al., 2019; Stoeber et al., 2018; Zhang et al., 2017).

The dendritic transport of nascent GPCRs can be mediated through multiple pathways (Choy et al., 2014; Liebmann et al., 2012; Valenzuela et al., 2014; Wei et al., 2021; Yudowski et al., 2006), direct interaction with regulatory proteins (Al Awabdh et al., 2012; Carrel et al., 2008; Doly et al., 2016; Zhang et al., 2016), and specific sequences embedded within the receptors (Carrel et al., 2006). In the canonical pathway, GPCRs are synthesized and post-translationally modified in the somatic endoplasmic reticulum (ER) and delivered to dendrites and synapses through lateral diffusion (Liebmann et al., 2012), as suggested for other types of receptors (Jacob et al., 2008; Triller and Choquet, 2005). However, secretory vesicles may participate in the

[1]Department of Pharmacology and Toxicology, Medical College of Georgia, Augusta University, Augusta, GA 30912, USA

[2]These authors contributed equally

[3]Lead contact

*Correspondence: guwu@augusta.edu

https://doi.org/10.1016/j.isci.2021.103643

dendritic transport of some GPCRs, such as serotonin 1B receptor (5-HT1B) (Wei et al., 2021) and α_2-adrenergic receptor (α_2-AR) (Liebmann et al., 2012). In addition, the local delivery involving the dendritic ER and Golgi outposts has been shown to be important for the dendritic delivery of γ-aminobutyric acid B receptor (GABABR) (Valenzuela et al., 2014). Among regulatory proteins identified are Yif1B for 5-HT1A (Carrel et al., 2008), PRAF2 (prenylated Rab acceptor 1 domain family member 2) for GABABR (Doly et al., 2016), and GGAs (Golgi-associated, γ-adaptin homologous, ARF-interacting proteins) and Rab43 for α_2-AR (Wei et al., 2021; Zhang et al., 2016). Both we and others have identified several highly conserved sequences which are crucial for the surface presentation of GPCRs in cell lines (Bermak et al., 2001; Dong et al., 2012; Dong and Wu, 2006; Duvernay et al., 2004, 2009a, 2009b; Janezic et al., 2020; Juhl et al., 2012; Robert et al., 2005; Schulein et al., 1998; Shiwarski et al., 2019; Walther et al., 2012). Among these motifs, the di-leucine (LL) motif located in the CT was shown to regulate 5-HT1A transport to dendrites in neurons (Carrel et al., 2006). However, virtually nothing is known about specific structural determinants required for GPCR targeting to the synaptic compartment.

Our laboratory has been interested in dissecting the molecular mechanisms that govern the anterograde transport of nascent GPCRs. The main purpose of this study is to investigate the structural basis of GPCR transport to dendrites and synapses in neurons, as well as their surface transport in cell lines, by focusing on prototypic family A α_2-AR, β-AR, and muscarinic acetylcholine receptor (mAChR). α_2-AR, β-AR, and mAChR have three (α_{2A}-AR, α_{2B}-AR, and α_{2C}-AR), three (β_1-AR, β_2-AR, and β_3-AR), and five subtypes (M1R–M5R), respectively, and all play important roles in the central and peripheral nervous systems. Here, we demonstrate that individual GPCRs may utilize distinct motifs, while different GPCRs use highly conserved sequences, to export to dendrites and post-synapses, and that motif-directed GPCR export trafficking may behave differently in neuronal and non-neuronal cells. These data provide important insights into the maturation processing and targeting to the functional destinations of the GPCR family in neurons.

RESULTS

Multiple motifs mediate α_{2B}-AR transport to the dendritic and post-synaptic compartments in hippocampal neurons

As an initial approach to searching for the intrinsic structural determinants for GPCR transport in neurons, we focused on specific motifs previously implicated in the export of α_{2B}-AR from the ER through the Golgi apparatus to the surface in cell lines. These motifs include the tyrosine-serine (YS) motif in the NT, a single leucine residue at position 48 (L48) in the center of the first intracellular loop (ICL1), a single phenylalanine residue at position 436 (F436) in the CT, and the isoleucine-leucine (IL) motif in the CT (Figure 1A). Our studies have shown that L48, F436, and the IL motif are involved in α_{2B}-AR export at the level of the ER, whereas the YS motif controls receptor exit from the Golgi apparatus (Dong and Wu, 2006; Duvernay et al., 2004, 2009a, 2009b). To define the role of these motifs in α_{2B}-AR transport to dendrites, α_{2B}-AR and its mutants were tagged with green fluorescent protein (GFP) at their CT and transiently expressed together with dsRed in primary cultures of hippocampal neurons. As accessed by the dsRed signal, expression of individual receptors did not significantly alter the general morphology of neurons. The spine length, width, and density were very much the same in neurons expressing α_{2B}-AR and its mutants (Data not shown).

Consistent with their functions in α_{2B}-AR transport in cell lines, mutation of YS, F436, and IL to alanines (A) markedly suppressed α_{2B}-AR expression at dendrites by greater than 65%, as compared with their wild-type (WT) counterpart (Figures 1B and 1C). Surprisingly, despite its remarkable inhibitory effect on the surface expression of α_{2B}-AR in cell lines (Duvernay et al., 2009a), L48 mutation had no effect on receptor transport to dendrites (Figures 1B and 1C). These data demonstrate that the functions of the YS motif, F436, and the IL motif are required for the dendritic targeting of α_{2B}-AR in hippocampal neurons.

We next determined the roles of these motifs in regulating α_{2B}-AR expression at the post-synaptic compartment. Mutation of YS, L48, F436, and IL each dramatically attenuated α_{2B}-AR presentation at dendritic spines. In particular, the effect of YS mutation was more profound in post-synapses than in dendrites, and the YS-AA mutant was almost completely unable to transport to post-synapses (Figures 2A and 2B). More interestingly, mutation of L48 caused substantial inhibition on α_{2B}-AR transport to the post-synaptic compartment by 75% (Figures 2A and 2B). Mutation of F436 and the IL motif similarly inhibited α_{2B}-AR transport to both dendrites and post-synapses. These data indicate that multiple motifs are involved in the biosynthesis of α_{2B}-AR in neurons.

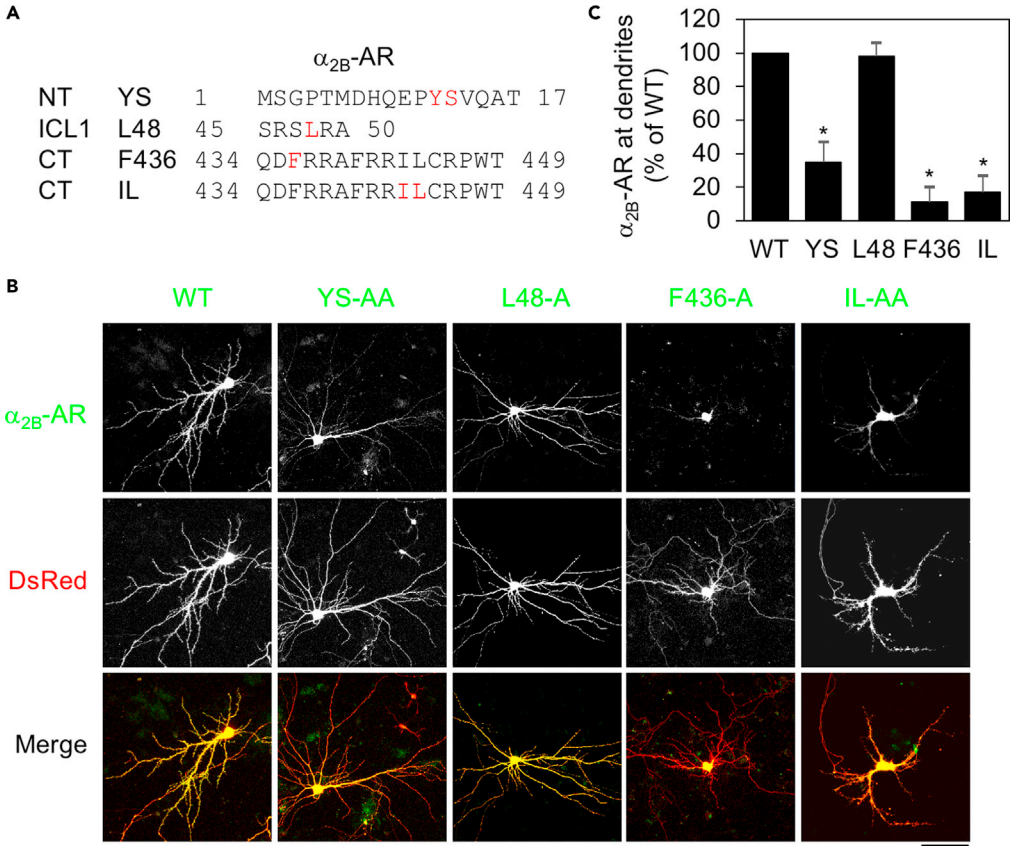

Figure 1. Mutation of YS, F436, and IL, but not L48, inhibits the dendritic transport of α_{2B}-AR in hippocampal neurons

(A) Positions of YS, L48, F436, and IL in α_{2B}-AR.

(B) The dendritic expression of α_{2B}-AR and its mutants. Hippocampal neurons were cultured and transfected with α_{2B}-AR-GFP or its mutants together with dsRed vectors for 48 h. After fixation, receptor expression was visualized by confocal microscopy. Scale bar, 50 μm.

(C) Quantitative data shown in (B). Dendritic receptor expression was defined as the dendritic area expressing the receptor. The data are expressed as percentages of WT. Bars represent mean ± SE (n = 6–12 neurons in at least 3 individual experiments). One-way ANOVA test; *p < 0.001 versus WT.

Differential motif-mediated transport of α_2-AR in neuronal and non-neuronal cells

Our preceding data suggest that individual motifs may have different effects on the dendritic and post-synaptic transport. These data, together with previous studies showing that GPCR transport along the secretory pathways may be different among primary neurons, neuronal cells, and non-neuronal cells (Daunt et al., 1997; Kim and von Zastrow, 2003; Kunselman et al., 2021; Shiwarski et al., 2019; Shiwarski et al., 2017a; Shiwarski et al., 2017b; Wei et al., 2021; Wozniak and Limbird, 1996, 1998), prompted us to determine if the motifs studied here could differentially influence the surface export of α_{2B}-AR in neuronal SHSY5Y and non-neuronal HEK293 cells. Our recent studies have shown that different GPCRs may use different pathways to transport to the cell surface in SHSY5Y cells (Wei et al., 2021). Radioligand binding assays and confocal microscopy showed that the L48, F436, and IL mutants were similarly arrested in the ER, unable to transport to the cell surface in HEK293 and SHSY5Y cells (Figures 3A, 3B, and S1). However, the subcellular localization of the YS mutant was clearly different in these two cell types. Whereas the YS mutant was largely expressed in the Golgi apparatus of HEK293 cells, it remained in the ER in SHSY5Y cells (Figures 3B and S1). Quantification using giantin and GM130 as Golgi markers showed that more than 70% of total YS-AA was colocalized with the Golgi in HEK293 cells, whereas only about 10% expressed at the Golgi in SHSY5Y cells (Figures 3C, 3E, S2A, and S2C).

As the YS motif is conserved in three α_2-ARs and, in addition to α_{2B}-AR, it is also important for α_{2A}-AR export (Dong and Wu, 2006), we compared the subcellular localization of the α_{2A}-AR YS-AA mutant in HEK293 and

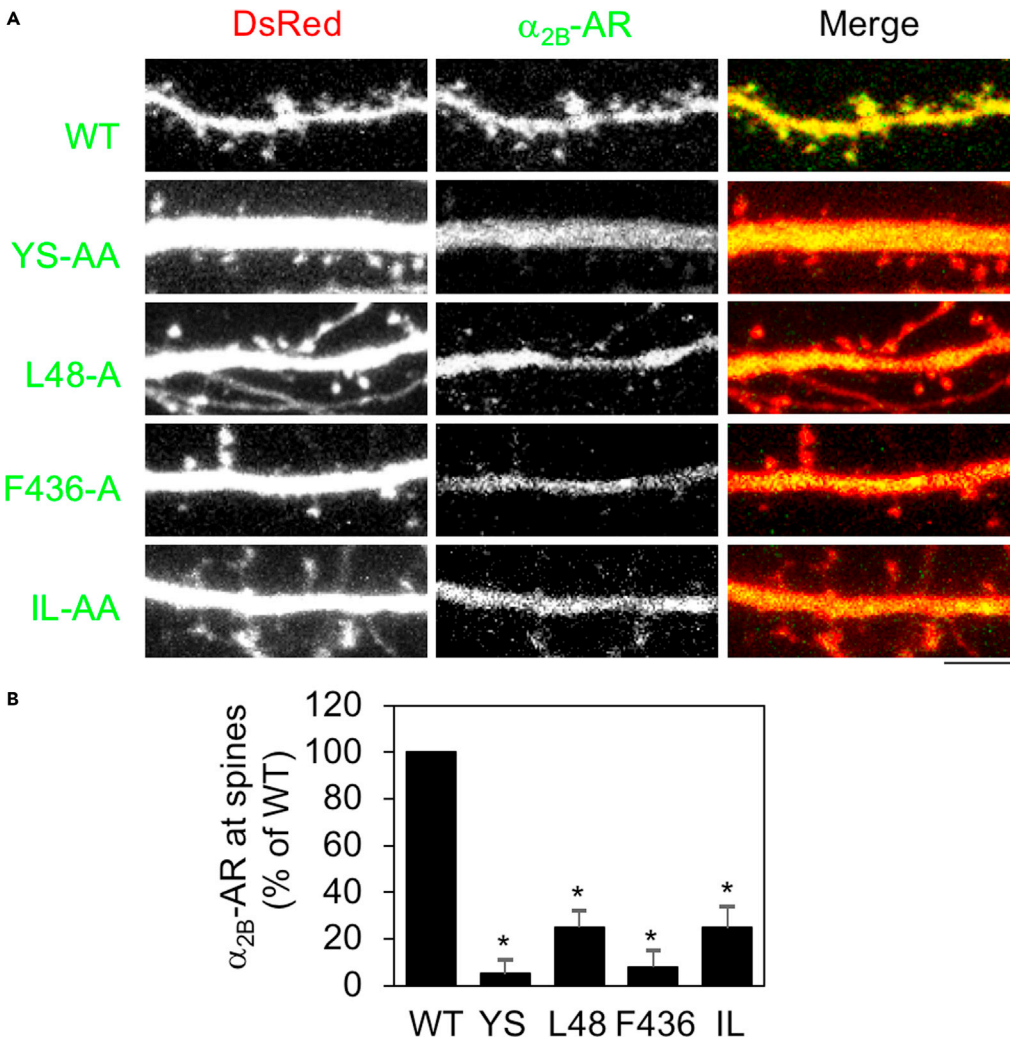

Figure 2. Mutation of YS, L48, F436, and IL inhibits the post-synaptic expression of α_{2B}-AR in hippocampal neurons

(A) The post-synaptic expression of α_{2B}-AR and its mutants. Scale bar, 5 μm.

(B) Quantitative data shown in (A). The post-synaptic receptor expression was defined by the ratio of spine over dendritic shaft expression. The data are expressed as percentages of WT. Bars represent mean ± SE (n = 30–50 spines in at least 3 separate experiments). One-way ANOVA test; *p < 0.001 versus WT.

SHSY5Y cells. Similar to the results observed with α_{2B}-AR, the YS mutant of α_{2A}-AR was mainly expressed in the Golgi of HEK293 cells, but extensively retained in the ER of SHSY5Y cells (Figures 3D, 3E, S2B, and S2C). These data suggest that the YS motif is able to differentially regulate α_2-AR transport between the ER and the Golgi in HEK293 and SHSY5Y cells.

The LL motif directs the dendritic and post-synaptic delivery of GPCRs in primary neurons

We next sought to determine if different GPCRs could use the same motifs to export in neurons. For this purpose, we focused on the LL motif in the dendritic and post-synaptic transport of β_2-AR and M3R (Figure 4A). The LL motif (L is leucine or isoleucine) is highly conserved in the C-terminal membrane-proximal region of family A GPCRs (Duvernay et al., 2004, 2009b). Similar to the effect of mutating the IL motif on α_{2B}-AR transport in neurons, mutation of the LL motif markedly reduced β_2-AR and M3R transport to dendrites (Figures 4B–4D). Mutation of the LL motif also dramatically inhibited the post-synaptic traffic of β_2-AR and M3R (Figures 4E–4G). The inhibitory effects of mutating the LL motif on the dendritic and post-synaptic transport of all three receptors were very much the same and, as compared with their respective WT

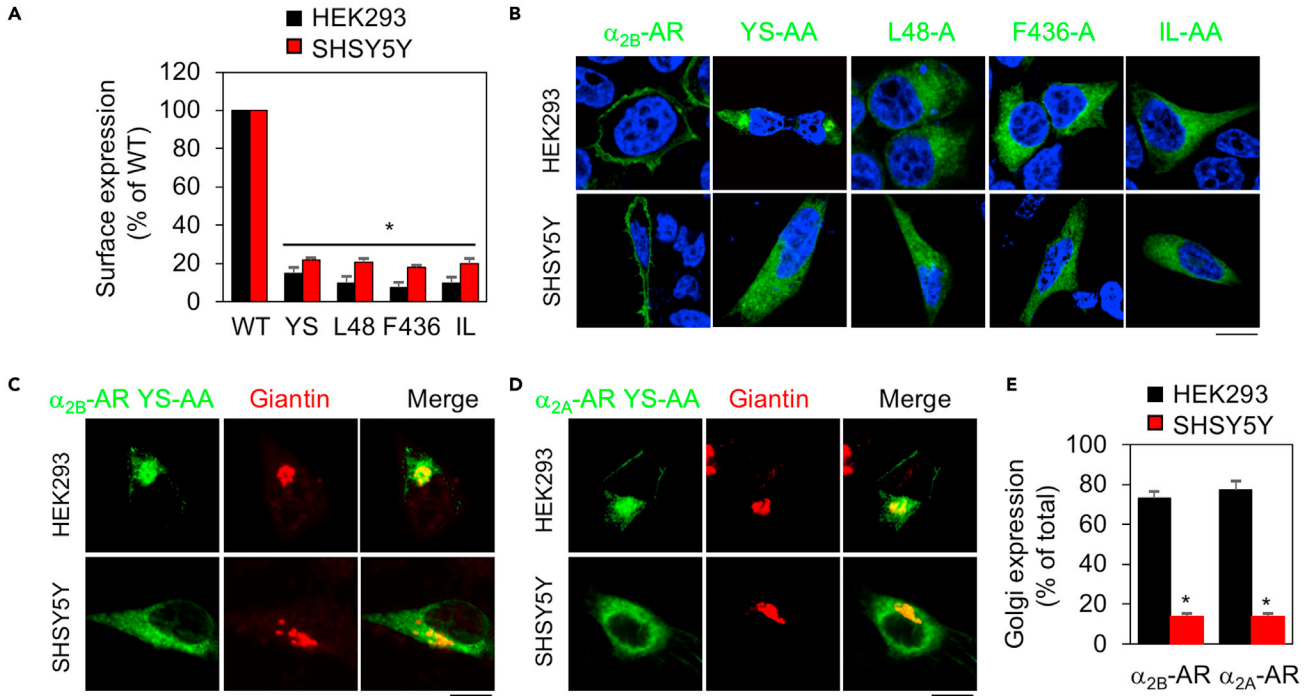

Figure 3. Surface expression and subcellular distribution of α_2-ARs and their mutants in HEK293 and SHSY5Y cells

(A) The expression of α_{2B}-AR and its mutants in HEK293 and SHSY5Y cells. The cells were transfected with α_{2B}-AR or individual mutants and their expression was measured by radioligand binding of intact live cells. The data are expressed as percentages of WT. Bars represent mean ± SE (n = 3). One-way ANOVA test; *p < 0.05 versus WT.

(B) Subcellular distribution of α_{2B}-AR and its mutants in HEK293 and SHSY5Y cells revealed by confocal microscopy. The images shown are representatives of 3 experiments. Scale bar, 10 μm.

(C) Colocalization of the YS-AA mutant of α_{2B}-AR with giantin in HEK293 and SHSY5Y cells. Scale bar, 10 μm.

(D) Colocalization of the YS-AA mutant of α_{2A}-AR with giantin in HEK293 and SHSY5Y cells. Scale bar, 10 μm.

(E) Quantitative data shown in (C) and (D). The data are expressed as percentages of total expression with a total of at least 20 cells quantified in each experiment. Bars represent mean ± SE (n = 3). Unpaired Student's t test; *p < 0.001 versus HEK293 cells.

receptors, the transport abilities of the mutated receptors were reduced by more than 75%. These data strongly suggest that the LL motif may function as a common code to direct GPCR transport to both dendritic and post-synaptic compartments in neurons.

The LL motif mediates the surface transport of wild-type and chimeric GPCRs in different cell types

The LL motif is known to control the surface transport of several GPCRs (Carrel et al., 2006; Duvernay et al., 2004, 2009b; Juhl et al., 2012; Robert et al., 2005; Sawyer et al., 2010; Schulein et al., 1998). However, its function in the biosynthesis of M3R has not been investigated. As such, we analyzed the effects of the LL motif on the surface expression and subcellular localization of M3R in HEK293 and SHSY5Y cells. Mutation of the LL motif remarkably blocked the surface transport of M3R as measured in intact cell-ligand binding assays (Figure 5A), and the M3R mutant LL-AA was colocalized with the ER marker DsRed-ER in both cell types (Figure 5B). In addition, mutating the LL motif produced the same effect on the cell surface transport and subcellular localization of β_2-AR in HEK293 and SHSY5Y cells (Figure S3).

To further define the role of the LL motif in mediating GPCR surface transport, we measured the effect of mutating the IL motif on the cell surface transport of the chimera $\beta_2AR\alpha_{2B}ct$ in which the β_2-AR CT containing 87 residues was substituted with the α_{2B}-AR CT containing 24 residues (Figure 5C). The chimeric $\beta_2AR\alpha_{2B}ct$ was expressed at the cell surface, whereas its IL mutant was strongly expressed in the ER in both HEK293 and SHSY5Y cells (Figure 5D).

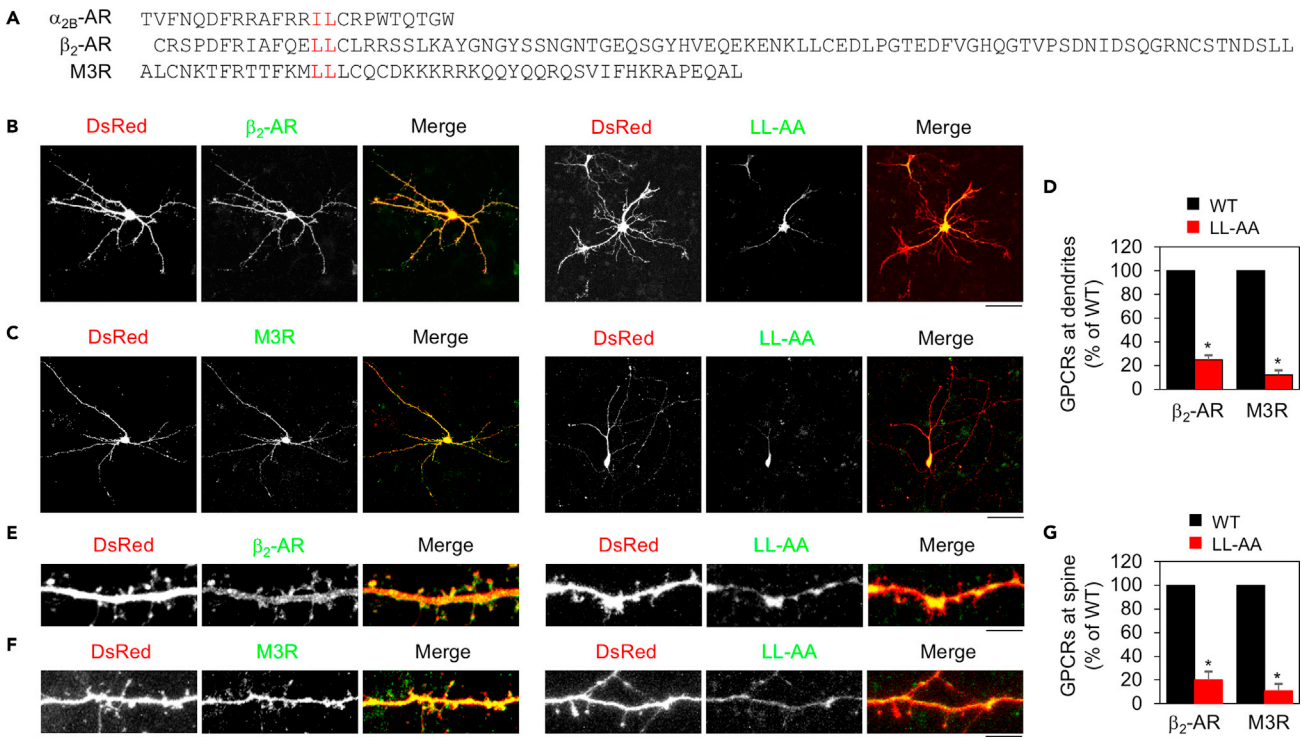

Figure 4. Mutation of the LL motif suppresses the dendritic and post-synaptic delivery of β_2-AR and M3R in hippocampal neurons

(A) Sequences of the CT of α_{2B}-AR, β_2-AR, and M3R.

(B) The dendritic expression of β_2-AR and its LL-AA mutant. Scale bar, 50 μm.

(C) The dendritic expression of M3R and its LL-AA mutant. Scale bar, 50 μm.

(D) Quantitative data shown in (B) and (C). The data are expressed as percentages of WT. Bars represent mean ± SE (n = 6–10 neurons in at least 3 experiments). Unpaired Student's t test; *p < 0.05 versus respective WT.

(E) The post-synaptic expression of β_2-AR and its LL-AA mutant. Scale bar, 5 μm.

(F) The post-synaptic expression of M3R and its LL-AA mutant. Scale bar, 5 μm.

(G) Quantitative data shown in (E) and (F). The data are expressed as percentages of WT. Bars represent mean ± SE (n = 30–50 spines in at least 3 experiments). Unpaired Student's t test; *p < 0.001 versus WT.

The LL motif confers its transport ability to vesicular stomatitis virus glycoprotein

We then determine if the LL motif of GPCRs could modulate the transport of non-GPCR plasma membrane proteins. For this purpose, we used a temperature-sensitive mutant of vesicular stomatitis virus glycoprotein (VSVGtsO45) which was misfolded and retained within the ER at restrictive temperature and correctly delivered to the Golgi at permissive temperature (Presley et al., 1997). We first generated two chimeras in which VSVG was fused at its CT with the entire C-terminus of α_{2B}-AR or β_2-AR. However, both chimeras did not export from the ER in HEK293 cells after culture at permissive temperature (data not shown). We then utilized the chimera VSVGct in which VSVG was conjugated to the helix 8 fragment G303-I320 of angiotensin II type 1 receptor (AT1R) (Figure 6A) (Li et al., 2017). This fragment contains an LL motif which mediates AT1R export from the ER (Duvernay et al., 2004; Zhang and Wu, 2019). Similar to VSVG, VSVGct was expressed and retained in the ER in cells cultured at 40°C and able to transport to the Golgi after shift to 32°C for 30 min in approximately 85% cells in both HEK293 and SHSY5Y cell types (Figures 6B and 6C). In marked contrast, the LL-AA mutant of VSVGct was remarkably arrested in the ER, unable to transport to the Golgi after incubation at 32°C for 30 min (Figures 6B and 6C).

We next determined if the LL motif of AT1R was able to facilitate the transport of a VSVG mutant lacking the DxE motif in the cytoplasmic CT (Figure 6D). The DxE motif is a well-characterized ER export motif which interacts with components of ER-derived COPII vesicles and thus, enhances VSVG export from the ER (Nishimura and Balch, 1997; Nishimura et al., 1999). Indeed, the DxE-AxA mutant of VSVG was extensively accumulated in the ER after incubation at 32°C for 30 min (Figures 6E and 6F). Addition of

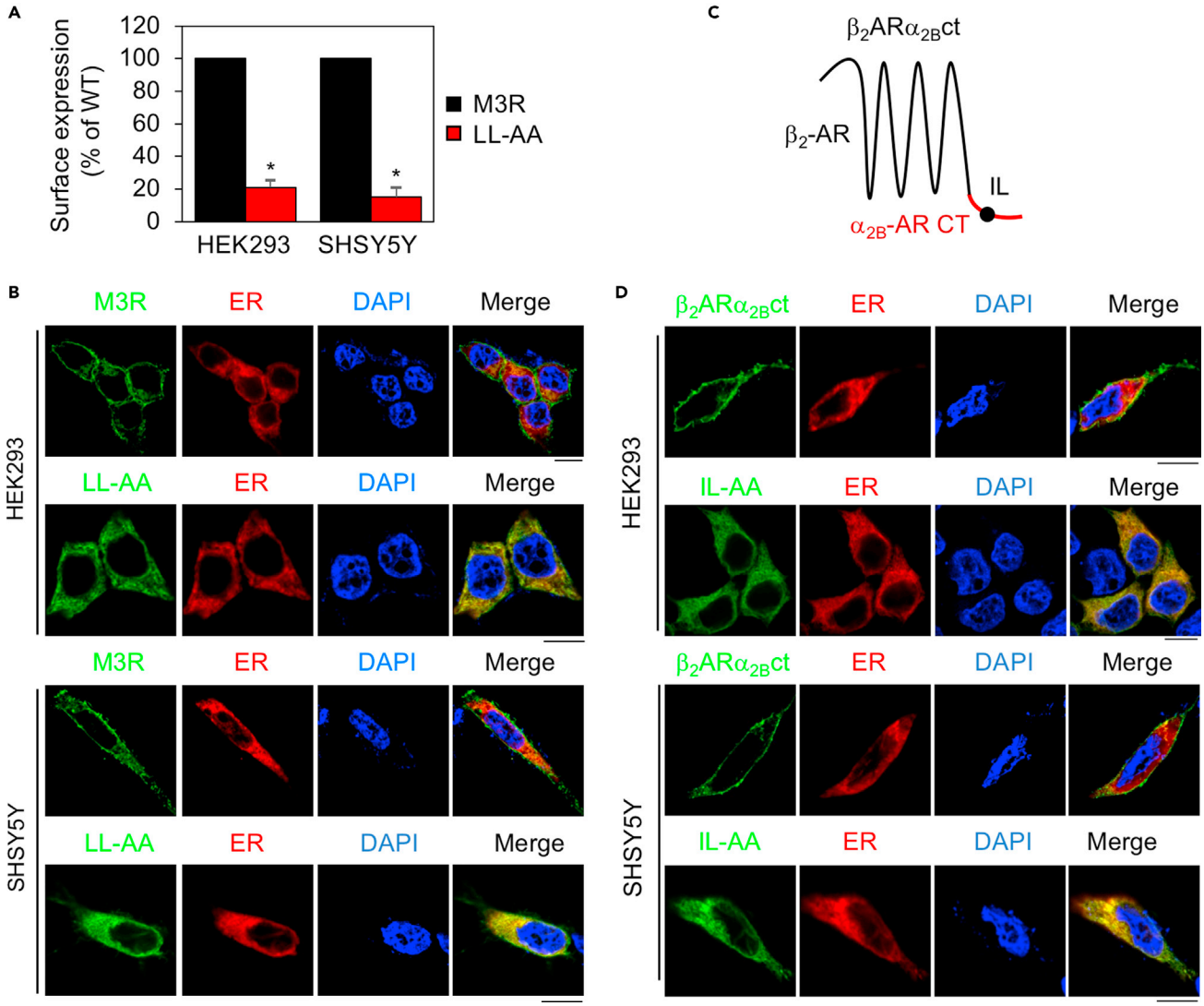

Figure 5. The LL motif mediates the surface transport from the ER of wild-type and chimeric GPCRs in HEK293 and SHSY5Y cells

(A) The surface expression of M3R and its LL-AA mutant. The cells were transfected with M3R or its mutant and their surface expression was measured by radioligand binding of intact live cells. The data are expressed as percentages of WT. Bars represent mean ± SE (n = 3). Unpaired Student's t test; *p < 0.001 versus WT.

(B) Subcellular distribution of M3R and its LL-AA mutant. M3R or its LL-AA mutant was transfected together with the ER marker DsRed-ER and their colocalization was revealed by confocal microscopy. The images shown are representatives of 3 experiments. Scale bar, 10 μm.

(C) A diagram showing the generation of the chimeric receptor β_2ARα_{2B}ct in which the β_2-AR CT was substituted with the α_{2B}-AR CT containing the IL motif.

(D) Subcellular distribution of β_2ARα_{2B}ct and its IL-AA mutant. β_2ARα_{2B}ct or its IL-AA mutant was transfected together with the ER marker DsRed-ER. The images shown are representatives of 3 experiments. Scale bar, 10 μm.

the AT1R CT strongly promoted the ER export of the VSVG DxE-AxA mutant and this effect of the AT1R CT was almost completely blocked by mutation of the LL motif (Figures 6E and 6F). These data suggest that the LL motif of AT1R is able to confer its transport ability to enhance the ER export of non-GPCR VSVG.

DISCUSSION

To define the intrinsic structural determinants for GPCR transport to dendritic spines in primary neurons, we have focused on the YS, L48, F436, and IL motifs of α_{2B}-AR. The most important finding of this paper is that L48 specifically regulates α_{2B}-AR delivery to the post-synaptic compartment without affecting dendritic transport (Figures 7A and 7B). Such striking disparities observed for a mutated GPCR to transport to

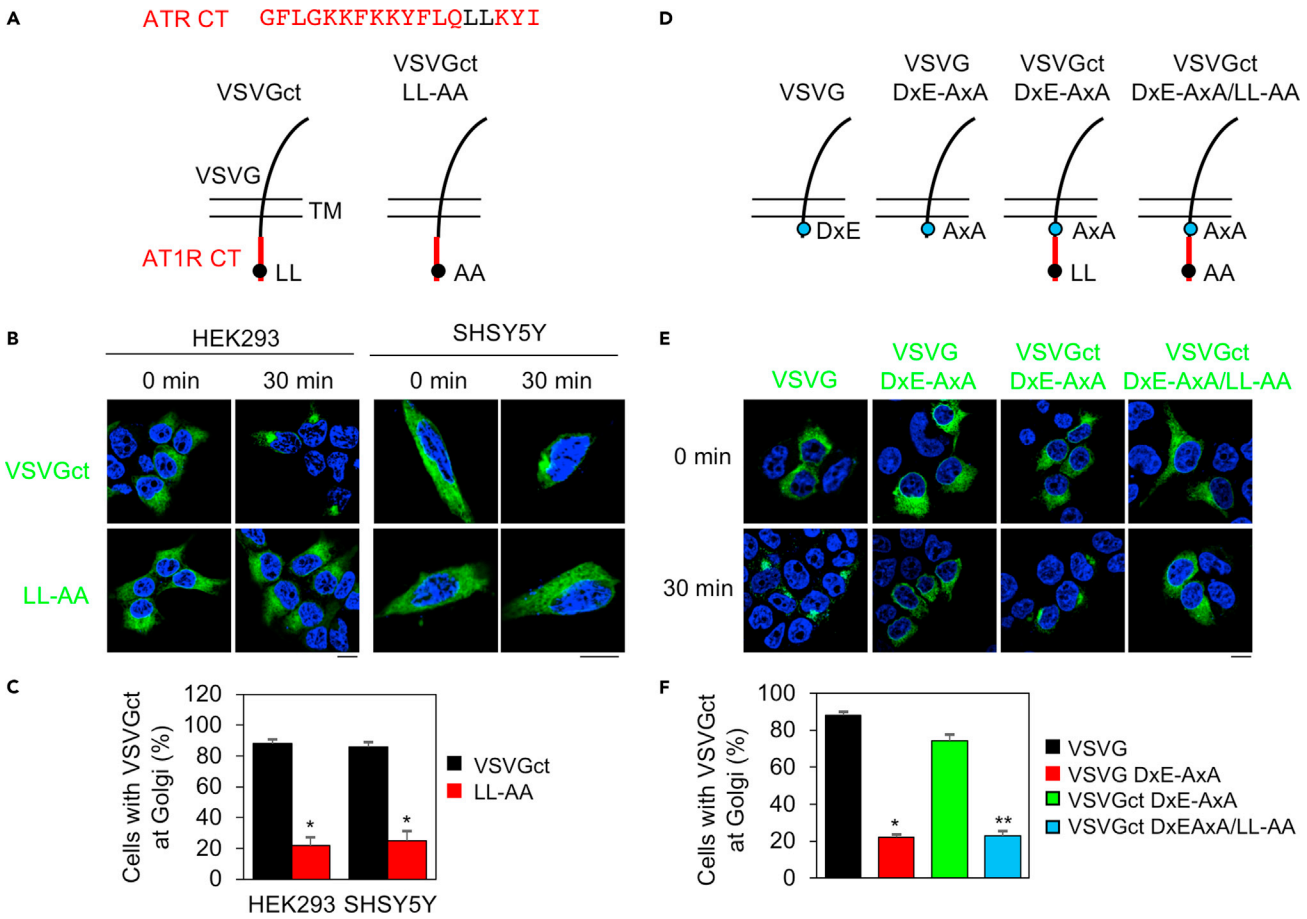

Figure 6. The LL motif of AT1R controls the ER export of VSVG

(A) A diagram showing the generation of the chimera VSVGct in which the C-terminal helical region of AT1R containing an LL motif (upper panel) was fused to the CT of VSVG (lower panel). TM, transmembrane domain.

(B) Subcellular distribution of VSVGct and its LL-AA mutant. HEK293 and SHSY5Y cells were transfected with GFP-tagged VSVGct or its LL-AA mutant. The cells were cultured at 40°C for 24 h (0 min) and then shifted to 32°C for 30 min. Scale bars, 10 μm.

(C) Quantitative data shown in (B). The data are expressed as percentages of the cells with VSVG expression at the Golgi with a total of at least 40 cells counted in each experiment. Bars represent mean ± SE (n = 3). Unpaired Student's t test; *p < 0.05 versus VSVGct.

(D) Diagrams showing the generation of VSVG and VSVGct mutants in which the DxE and/or LL motifs were mutated to alanines.

(E) Subcellular distribution of VSVG and VSVGct mutants. Scale bar, 10 μm.

(F) Quantitative data shown in (E). The data are expressed as percentages of the cells with VSVG expression at the Golgi with a total of at least 40 cells counted in each experiment. Bars represent mean ± SE (n = 3). Unpaired Student's t test; *p < 0.001 versus VSVG; **p < 0.001 versus VSVGct DxE-AxA.

dendrites and post-synapses are surprising and have several important implications. First, as α_{2B}-AR transport in neurons is regulated by Rab8, Rab43, and GGAs (Dong et al., 2010a; Wei et al., 2021; Zhang et al., 2016), secretory vesicles are likely involved in its forward delivery. Therefore, it is highly possible that α_{2B}-AR forward trafficking along dendrites uses both canonical lateral diffusion and non-canonical, active vesicle-mediated secretory pathway (Figure 7A) as suggested for 5-HT1B (Wei et al., 2021). The fact that L48 specifically regulates α_{2B}-AR delivery to the post-synaptic compartment implies distinct mechanisms by which individual GPCRs target to dendrites and post-synapses; second, GPCR transport to post-synapses is a highly selective process; third, it is possible that the residue L48 may specifically regulate a unique yet unknown secretory pathway that delivers nascent α_{2B}-AR to the post-synaptic compartment. This possibility is supported by the fact that multiple secretory routes may exist to deliver GPCRs in neurons, including the local pathway through the dendritic ER and Golgi outposts (Choy et al., 2014; Liebmann et al., 2012; Valenzuela et al., 2014; Wei et al., 2021; Yudowski et al., 2006); fourth, these data also provide important evidence indicating that the trafficking function of L48 is unlikely mediated through regulating proper receptor folding which presumably affects dendritic trafficking as well.

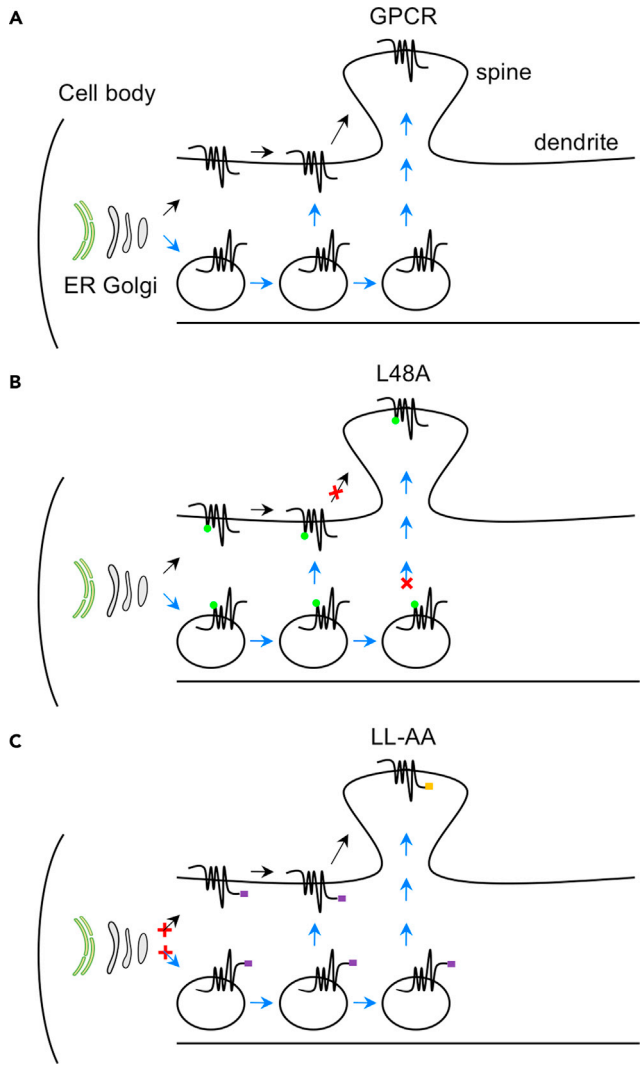

Figure 7. Diagrams showing the function of specific motifs in GPCR transport in neurons

(A) GPCR transport to the dendritic and post-synaptic compartments through lateral diffusion (black arrow) and secretory vesicle-mediated pathway (blue arrow).

(B) Mutation of L48 on the ICL1 specifically disrupts post-synaptic transport. X indicates the position where the mutated receptors are unable to move forward.

(C) Mutation of the LL motif in the CT blocks dendritic and post-synaptic transport from the cell body where the receptors are synthesized.

Another important finding presented here is that the LL motif may function as a common export signal to direct GPCR transport to dendrites and post-synapses in neurons (Figure 7C). This became evident as mutation of the LL motif almost abolished the dendritic and post-synaptic expression of all GPCRs studied, albeit these receptors may use distinct pathways (Wei et al., 2021). Such an obligatory role of the LL motif is also reflected by the fact that its mutation disrupts the ER export of several GPCRs (Carrel et al., 2006; Duvernay et al., 2004, 2009b; Robert et al., 2005; Sawyer et al., 2010; Schulein et al., 1998) and the chimera β_2ARα_{2B}CT in different cell lines. Because the LL motif is located in the membrane-proximal C-terminal α-helical region, its mutation will likely disrupt proper receptor folding in the ER (Robert et al., 2005; Schulein et al., 1998). Therefore, no matter the trafficking pathways they utilize, the mutated receptors are unable to export from the cell body where they are synthesized (Figure 7C). However, structural analysis shows that the side chains of LL residues are exposed to the cytosolic space in the receptor's native environment (Duvernay et al., 2009b; Rosenbaum et al., 2007), suggesting that the LL motif may function as an ER export motif or mediate receptor interaction with some proteins to direct receptor export from the ER. In support of these possibilities, the LL motif identified in the AT1R CT is able to

control the ER export of both wild-type VSVG and its ER export-deficient mutant as demonstrated in this study. In addition, the LL motif mediates β_2-AR interaction with Rab8 and Rab1 (Dong et al., 2010a; Hammad et al., 2012), small GTPases involved in the post-Golgi and ER transport of GPCRs, respectively (Deretic et al., 1995; Filipeanu et al., 2004, 2006; Wang and Wu, 2012; Wu et al., 2003), further suggesting that the LL motif may have multiple functions in directing GPCR forward trafficking.

This study has also revealed that the N-terminally located YS motif represents an important factor to control differential trafficking and subcellular distribution of α_2-ARs in different cell types. In comparison of motif-directed GPCR traffic in neuronal SHSY5Y and non-neuronal HEK293 cells, we have found that, although α_{2A}-AR and α_{2B}-AR robustly express at the cell surface and their surface expression is clearly disrupted by mutation of the YS motif in SHSY5Y and HEK293 cells, distribution of the YS-AA mutant into the ER and Golgi compartments at steady state is substantially different in these two cell types. In addition, YS mutation causes more deleterious effects on α_{2B}-AR transport to post-synapses than dendrites. These data are consistent with previous studies showing different maturation processing of some GPCRs, such as α_2-ARs (Daunt et al., 1997; Wei et al., 2021; Wozniak and Limbird, 1996, 1998) and opioid receptors (Kim and von Zastrow, 2003; Kunselman et al., 2021; Shiwarski et al., 2019; Shiwarski et al., 2017a; Shiwarski et al., 2017b), in terms of their subcellular localization patterns and export trafficking itineraries in different cell types. It is possible that the YS mutant is somewhat better in export from the ER in HEK293 cells than SHSY5Y cells. Alternatively, more ER accumulation of the YS mutant in SHSY5Y cells may be due to enhanced retrograde transport from the Golgi where the mutated receptors are unable to export forward to the surface. Nevertheless, these data suggest that the YS motif may dictate α_2-AR export from distinct early secretory compartments (i.e. ER and Golgi) in different cell types. However, whether such YS motif-mediated cell-type-selective regulation is commonly shared by other neuronal and non-neuronal cells needs further investigation.

Despite their well-defined importance in controlling neuronal function and as drug targets of numerous neurological disorders, the synaptic targeting of GPCRs is poorly studied and the players involved in GPCR biosynthesis in neurons have just begun to be revealed. This study has demonstrated that while individual GPCRs may utilize distinct sequences for their targeting to dendrites and synapses, different GPCRs may share common motifs for export trafficking. These data, together with previous studies, indicate the complexity of GPCR trafficking along the anterograde pathways in sophisticated neurons. As failure of GPCR transport to the functional destinations is clearly associated with the pathogenesis of neurological disorders, further elucidation of how GPCR forward trafficking is achieved in neurons may help design therapeutic strategies for these diseases by targeting GPCR biosynthetic processing.

Limitations of the study

Future work needs to study the targeting and biosynthesis of GPCRs at endogenous levels in primary neurons and cell lines.

STAR★METHODS

Detailed methods are provided in the online version of this paper and include the following:

- KEY RESOURCES TABLE
- RESOURCE AVAILABILITY
  - Lead contact
  - Materials availability
  - Data and code availability
- EXPERIMENTAL MODELS AND SUBJECT DETAILS
  - Cell culture
  - Preparation of primary neurons
  - Animals
- METHOD DETAILS
  - Plasmid constructions
  - Transient transfection
  - Fluorescence microscopy
  - Radioligand binding of intact live cells
  - Measurement of VSVG transport from the ER to the Golgi
- QUANTIFICATION AND STATISTICAL ANALYSIS

SUPPLEMENTAL INFORMATION

Supplemental information can be found online at https://doi.org/10.1016/j.isci.2021.103643.

ACKNOWLEDGMENTS

This work was supported by the NIH, United States (grants R35GM136397 and R01GM118915 to G.W.).

AUTHOR CONTRIBUTIONS

X.X., Z.W., and G.W. conceived and designed the experiments. X.X. and Z.W. performed the experiments. X.X., Z.W., and G.W. analyzed the results. X.X. and G.W. wrote the manuscript.

DECLARATION OF INTEREST

The authors declare no competing interests.

Received: October 1, 2021
Revised: November 19, 2021
Accepted: December 14, 2021
Published: January 21, 2022

REFERENCES

Al Awabdh, S., Miserey-Lenkei, S., Bouceba, T., Masson, J., Kano, F., Marinach-Patrice, C., Hamon, M., Emerit, M.B., and Darmon, M. (2012). A new vesicular scaffolding complex mediates the G-protein-coupled 5-HT1A receptor targeting to neuronal dendrites. J. Neurosci. *32*, 14227–14241.

Bermak, J.C., Li, M., Bullock, C., and Zhou, Q.Y. (2001). Regulation of transport of the dopamine D1 receptor by a new membrane-associated ER protein. Nat.Cell Biol. *3*, 492–498.

Betke, K.M., Wells, C.A., and Hamm, H.E. (2012). GPCR mediated regulation of synaptic transmission. Prog.Neurobiol. *96*, 304–321.

Carrel, D., Hamon, M., and Darmon, M. (2006). Role of the C-terminal di-leucine motif of 5-HT1A and 5-HT1B serotonin receptors in plasma membrane targeting. J.Cell Sci. *119*, 4276–4284.

Carrel, D., Masson, J., Al Awabdh, S., Capra, C.B., Lenkei, Z., Hamon, M., Emerit, M.B., and Darmon, M. (2008). Targeting of the 5-HT1A serotonin receptor to neuronal dendrites is mediated by Yif1B. J. Neurosci. *28*, 8063–8073.

Chen, Y., Peng, Y., Che, P., Gannon, M., Liu, Y., Li, L., Bu, G., van Groen, T., Jiao, K., and Wang, Q. (2014). alpha(2A) adrenergic receptor promotes amyloidogenesis through disrupting APP-SorLA interaction. Proc. Natl. Acad. Sci. U S A *111*, 17296–17301.

Choy, R.W., Park, M., Temkin, P., Herring, B.E., Marley, A., Nicoll, R.A., and von Zastrow, M. (2014). Retromer mediates a discrete route of local membrane delivery to dendrites. Neuron *82*, 55–62.

Daunt, D.A., Hurt, C., Hein, L., Kallio, J., Feng, F., and Kobilka, B.K. (1997). Subtype-specific intracellular trafficking of alpha2-adrenergic receptors. Mol. Pharmacol. *51*, 711–720.

Deretic, D., Huber, L.A., Ransom, N., Mancini, M., Simons, K., and Papermaster, D.S. (1995). rab8 in retinal photoreceptors may participate in rhodopsin transport and in rod outer segment disk morphogenesis. J.Cell Sci. *108*, 215–224.

Doly, S., Shirvani, H., Gata, G., Meye, F.J., Emerit, M.B., Enslen, H., Achour, L., Pardo-Lopez, L., Yang, S.K., Armand, V., et al. (2016). GABAB receptor cell-surface export is controlled by an endoplasmic reticulum gatekeeper. Mol. Psychiatry *21*, 480–490.

Dong, C., Filipeanu, C.M., Duvernay, M.T., and Wu, G. (2007). Regulation of G protein-coupled receptor export trafficking. Biochim.Biophys. Acta *1768*, 853–870.

Dong, C., Nichols, C.D., Guo, J., Huang, W., Lambert, N.A., and Wu, G. (2012). A triple arg motif mediates alpha(2B)-adrenergic receptor interaction with Sec24C/D and export. Traffic *13*, 857–868.

Dong, C., and Wu, G. (2006). Regulation of anterograde transport of alpha2-adrenergic receptors by the N termini at multiple intracellular compartments. J. Biol. Chem. *281*, 38543–38554.

Dong, C., Yang, L., Zhang, X., Gu, H., Lam, M.L., Claycomb, W.C., Xia, H., and Wu, G. (2010a). Rab8 interacts with distinct motifs in alpha2B- and beta2-adrenergic receptors and differentially modulates their transport. J. Biol. Chem. *285*, 20369–20380.

Dong, C., Zhang, X., Zhou, F., Dou, H., Duvernay, M.T., Zhang, P., and Wu, G. (2010b). ADP-ribosylation factors modulate the cell surface transport of G protein-coupled receptors. J. Pharmacol. Exp. Ther. *333*, 174–183.

Duvernay, M.T., Zhou, F., and Wu, G. (2004). A conserved motif for the transport of G protein-coupled receptors from the endoplasmic reticulum to the cell surface. J. Biol. Chem. *279*, 30741–30750.

Duvernay, M.T., Dong, C., Zhang, X., Robitaille, M., Hebert, T.E., and Wu, G. (2009a). A single conserved leucine residue on the first intracellular loop regulates ER export of G protein-coupled receptors. Traffic *10*, 552–566.

Duvernay, M.T., Dong, C., Zhang, X., Zhou, F., Nichols, C.D., and Wu, G. (2009b). Anterograde trafficking of G protein-coupled receptors: function of the C-terminal F(X)6LL motif in export from the endoplasmic reticulum. Mol. Pharmacol. *75*, 751–761.

Filipeanu, C.M., Zhou, F., Claycomb, W.C., and Wu, G. (2004). Regulation of the cell surface expression and function of angiotensin II type 1 receptor by Rab1-mediated endoplasmic reticulum-to-Golgi transport in cardiac myocytes. J. Biol. Chem. *279*, 41077–41084.

Filipeanu, C.M., Zhou, F., Fugetta, E.K., and Wu, G. (2006). Differential regulation of the cell-surface targeting and function of beta- and alpha1-adrenergic receptors by Rab1 GTPase in cardiac myocytes. Mol. Pharmacol. *69*, 1571–1578.

Gainetdinov, R.R., Premont, R.T., Bohn, L.M., Lefkowitz, R.J., and Caron, M.G. (2004). Desensitization of G protein-coupled receptors and neuronal functions. Annu. Rev. Neurosci. *27*, 107–144.

Hammad, M.M., Kuang, Y.Q., Morse, A., and Dupre, D.J. (2012). Rab1 interacts directly with the beta2-adrenergic receptor to regulate receptor anterograde trafficking. Biol. Chem. *393*, 541–546.

Jacob, T.C., Moss, S.J., and Jurd, R. (2008). GABA(A) receptor trafficking and its role in the dynamic modulation of neuronal inhibition. Nat. Rev. Neurosci. *9*, 331–343.

Janezic, E.M., Lauer, S.M., Williams, R.G., Chungyoun, M., Lee, K.S., Navaluna, E., Lau, H.T., Ong, S.E., and Hague, C. (2020). N-glycosylation of alpha1D-adrenergic receptor N-terminal domain is required for correct trafficking, function, and biogenesis. Sci.Rep. *10*, 7209.

Juhl, C., Kosel, D., and Beck-Sickinger, A.G. (2012). Two motifs with different function regulate the anterograde transport of the adiponectin receptor 1. Cell. Signal. *24*, 1762–1769.

Kim, K.A., and von Zastrow, M. (2003). Neurotrophin-regulated sorting of opioid receptors in the biosynthetic pathway of neurosecretory cells. J. Neurosci. *23*, 2075–2085.

Kunselman, J.M., Lott, J., and Puthenveedu, M.A. (2021). Mechanisms of selective G protein-coupled receptor localization and trafficking. Curr.Opin.Cell Biol. *71*, 158–165.

Li, C., Fan, Y., Lan, T.H., Lambert, N.A., and Wu, G. (2012). Rab26 modulates the cell surface transport of alpha2-adrenergic receptors from the Golgi. J. Biol. Chem. *287*, 42784–42794.

Li, C., Wei, Z., Fan, Y., Huang, W., Su, Y., Li, H., Dong, Z., Fukuda, M., Khater, M., and Wu, G. (2017). The GTPase Rab43 controls the anterograde ER-Golgi trafficking and sorting of GPCRs. Cell Rep. *21*, 1089–1101.

Liebmann, T., Kruusmagi, M., Sourial-Bassillious, N., Bondar, A., Svenningsson, P., Flajolet, M., Greengard, P., Scott, L., Brismar, H., and Aperia, A. (2012). A noncanonical postsynaptic transport route for a GPCR belonging to the serotonin receptor family. J. Neurosci. *32*, 17998–18008.

Lyssand, J.S., Whiting, J.L., Lee, K.S., Kastl, R., Wacker, J.L., Bruchas, M.R., Miyatake, M., Langeberg, L.K., Chavkin, C., Scott, J.D., et al. (2010). Alpha-dystrobrevin-1 recruits alpha-catulin to the alpha1D-adrenergic receptor/dystrophin-associated protein complex signalosome. Proc. Natl. Acad. Sci. U S A *107*, 21854–21859.

Nishimura, N., and Balch, W.E. (1997). A di-acidic signal required for selective export from the endoplasmic reticulum. Science *277*, 556–558.

Nishimura, N., Bannykh, S., Slabough, S., Matteson, J., Altschuler, Y., Hahn, K., and Balch, W.E. (1999). A di-acidic (DXE) code directs concentration of cargo during export from the endoplasmic reticulum. J. Biol. Chem. *274*, 15937–15946.

Pierce, K.L., Premont, R.T., and Lefkowitz, R.J. (2002). Seven-transmembrane receptors. Nat. Rev. Mol.Cell Biol. *3*, 639–650.

Presley, J.F., Cole, N.B., Schroer, T.A., Hirschberg, K., Zaal, K.J.M., and LippincottSchwartz, J. (1997). ER-to-Golgi transport visualized in living cells. Nature *389*, 81–85.

Retamal, J.S., Ramirez-Garcia, P.D., Shenoy, P.A., Poole, D.P., and Veldhuis, N.A. (2019). Internalized GPCRs as potential therapeutic targets for the management of pain. Front.Mol.Neurosci. *12*, 273.

Robert, J., Clauser, E., Petit, P.X., and Ventura, M.A. (2005). A novel C-terminal motif is necessary for the export of the vasopressin V1b/V3 receptor to the plasma membrane. J. Biol. Chem. *280*, 2300–2308.

Rosenbaum, D.M., Cherezov, V., Hanson, M.A., Rasmussen, S.G., Thian, F.S., Kobilka, T.S., Choi, H.J., Yao, X.J., Weis, W.I., Stevens, R.C., et al. (2007). GPCR engineering yields high-resolution structural insights into beta2-adrenergic receptor function. Science *318*, 1266–1273.

Roth, B.L. (2019). Molecular pharmacology of metabotropic receptors targeted by neuropsychiatric drugs. Nat. Struct. Mol. Biol. *26*, 535–544.

Sawyer, G.W., Ehlert, F.J., and Shults, C.A. (2010). A conserved motif in the membrane proximal C-terminal tail of human muscarinic m1 acetylcholine receptors affects plasma membrane expression. J. Pharmacol. Exp. Ther. *332*, 76–86.

Schulein, R., Hermosilla, R., Oksche, A., Dehe, M., Wiesner, B., Krause, G., and Rosenthal, W. (1998). A dileucine sequence and an upstream glutamate residue in the intracellular carboxyl terminus of the vasopressin V2 receptor are essential for cell surface transport in COS.M6 cells. Mol. Pharmacol. *54*, 525–535.

Shiwarski, D.J., Crilly, S.E., Dates, A., and Puthenveedu, M.A. (2019). Dual RXR motifs regulate nerve growth factor-mediated intracellular retention of the delta opioid receptor. Mol. Biol.Cell *30*, 680–690.

Shiwarski, D.J., Darr, M., Telmer, C.A., Bruchez, M.P., and Puthenveedu, M.A. (2017a). PI3K class II alpha regulates delta-opioid receptor export from the trans-Golgi network. Mol. Biol.Cell *28*, 2202–2219.

Shiwarski, D.J., Tipton, A., Giraldo, M.D., Schmidt, B.F., Gold, M.S., Pradhan, A.A., and Puthenveedu, M.A. (2017b). A PTEN-regulated checkpoint controls surface delivery of delta opioid receptors. J. Neurosci. *37*, 3741–3752.

Stoeber, M., Jullie, D., Lobingier, B.T., Laeremans, T., Steyaert, J., Schiller, P.W., Manglik, A., and von Zastrow, M. (2018). A genetically encoded biosensor reveals location bias of opioid drug action. Neuron *98*, 963–976 e965.

Triller, A., and Choquet, D. (2005). Surface trafficking of receptors between synaptic and extrasynaptic membranes: and yet they do move! Trends Neurosci. *28*, 133–139.

Valenzuela, J.I., Jaureguiberry-Bravo, M., Salas, D.A., Ramirez, O.A., Cornejo, V.H., Lu, H.E., Blanpied, T.A., and Couve, A. (2014). Transport along the dendritic endoplasmic reticulum mediates the trafficking of GABAB receptors. J.Cell Sci. *127*, 3382–3395.

Walther, C., Lotze, J., Beck-Sickinger, A.G., and Morl, K. (2012). The anterograde transport of the human neuropeptide Y2 receptor is regulated by a subtype specific mechanism mediated by the C-terminus. Neuropeptides *46*, 335–343.

Wang, G., and Wu, G. (2012). Small GTPase regulation of GPCR anterograde trafficking. Trends Pharmacol. Sci. *33*, 28–34.

Wang, Q., Zhao, J.L., Brady, A.E., Feng, J., Allen, P.B., Lefkowitz, R.J., Greengard, P., and Limbird, L.E. (2004). Spinophilin blocks arrestin actions in vitro and in vivo at G protein-coupled receptors. Science *304*, 1940–1944.

Wei, Z., Zhang, M., Li, C., Huang, W., Fan, Y., Guo, J., Khater, M., Fukuda, M., Dong, Z., Hu, G., et al. (2019). Specific TBC omain-containing proteins control the ER-Golgi-plasma membrane trafficking of GPCRs. Cell Rep. *28*, 554–566 e554.

Wei, Z., Xu, X., Fang, Y., Khater, M., Naughton, S.X., Hu, G., Terry, A.V., Jr., and Wu, G. (2021). Rab43 GTPase directs postsynaptic trafficking and neuron-specific sorting of G protein-coupled receptors. J. Biol. Chem. *296*, 100517.

Weinberg, Z.Y., Crilly, S.E., and Puthenveedu, M.A. (2019). Spatial encoding of GPCR signaling in the nervous system. Curr.Opin.Cell Biol. *57*, 83–89.

Wess, J. (1997). G-protein-coupled receptors: molecular mechanisms involved in receptor activation and selectivity of G-protein recognition. FASEB J. *11*, 346–354.

Wozniak, M., and Limbird, L.E. (1996). The three alpha 2-adrenergic receptor subtypes achieve basolateral localization in Madin-Darby canine kidney II cells via different targeting mechanisms. J. Biol. Chem. *271*, 5017–5024.

Wozniak, M., and Limbird, L.E. (1998). Trafficking itineraries of G protein-coupled receptors in epithelial cells do not predict receptor localization in neurons. Brain Res. *780*, 311–322.

Wu, G., Benovic, J.L., Hildebrandt, J.D., and Lanier, S.M. (1998). Receptor docking sites for G-protein betagamma subunits.Implications for signal regulation. J. Biol. Chem. *273*, 7197–7200.

Wu, G., Krupnick, J.G., Benovic, J.L., and Lanier, S.M. (1997). Interaction of arrestins with intracellular domains of muscarinic and alpha2-adrenergic receptors. J. Biol. Chem. *272*, 17836–17842.

Wu, G., Zhao, G., and He, Y. (2003). Distinct pathways for the trafficking of angiotensin II and adrenergic receptors from the endoplasmic reticulum to the cell surface: rab1-independent transport of a G protein-coupled receptor. J.Biol.Chem. *278*, 47062–47069.

Yudowski, G.A., Puthenveedu, M.A., and von Zastrow, M. (2006). Distinct modes of regulated receptor insertion to the somatodendritic plasma membrane. Nat. Neurosci. *9*, 622–627.

Zhang, F., Gannon, M., Chen, Y., Zhou, L., Jiao, K., and Wang, Q. (2017). The amyloid precursor protein modulates alpha2A-adrenergic receptor endocytosis and signaling through disrupting arrestin 3 recruitment. FASEB J. *31*, 4434–4446.

Zhang, M., Huang, W., Gao, J., Terry, A.V., and Wu, G. (2016). Regulation of alpha2B-adrenergic receptor cell surface transport by GGA1 and GGA2. Sci.Rep. *6*, 37921.

Zhang, M., and Wu, G. (2019). Mechanisms of the anterograde trafficking of GPCRs: regulation of AT1R transport by interacting proteins and motifs. Traffic *20*, 110–120.

STAR★METHODS

KEY RESOURCES TABLE

REAGENT or RESOURCE	SOURCE	IDENTIFIER
Antibodies		
Mouse monoclonal anti-GM130 (clone 35)	BD Biosciences	610823
Rabbit polyclonal anti-giantin	Abcam	ab80864
Goat anti-rabbit IgG (H+L), Alexa Fluor 594	Thermo Fisher Scientific	A-11012
Goat anti-mouse IgG (H+L), Alexa Fluor 594	Thermo Fisher Scientific	A-11032
Chemicals, peptides, and recombinant proteins		
[^{3}H]-RX821002	Perkin-Elmer	NET1153250UC
[^{3}H]-CGP12177	Perkin-Elmer	NET1061250UC
[N-methyl-^{3}H]-scopolamine methyl chloride	Perkin-Elmer	NET636250UC
Lipofectamine 2000	Thermo Fisher Scientific	11668019
Dulbecco's modified eagles medium	HyClone	SH30243.01HI
Ham's F-12 nutrient mix	Thermo Fisher Scientific	11765054
Minimum essential medium	Thermo Fisher Scientific	11095080
Neurobasal-A medium	Thermo Fisher Scientific	12349015
B-27 supplement	Thermo Fisher Scientific	17504001
GlutaMax supplement	Thermo Fisher Scientific	35050061
Fetal bovine serum	HyClone	SH30396.03HI
Penicillin-streptomycin solution	HyClone	SV30010
ProLong gold antifade mountant with DAPI	Invitrogen	P36931
Experimental models: Cell lines		
HEK293	ATCC	CRL-1573
SHSY5Y	ATCC	CRL-2266
Sprague-Dawley rats	Charles River Laboratories	
Primers (Table S1)	This paper	N/A
Recombinant DNA		
α_{2B}-AR-GFP	(Wu et al., 2003)	N/A
α_{2B}-AR YS-AA-GFP	(Dong and Wu, 2006)	N/A
α_{2B}-AR L48-A-GFP	(Duvernay et al., 2009a)	N/A
α_{2B}-AR F436-A-GFP	(Duvernay et al., 2004)	N/A
α_{2B}-AR IL-AA-GFP	(Duvernay et al., 2004)	N/A
β_2-AR-GFP	(Wu et al., 2003)	N/A
β_2-AR LL-AA-GFP	(Duvernay et al., 2009a)	N/A
β_2ARα2ct-GFP	(Dong et al., 2010a)	N/A
β_2ARα2ct IL-AA-GFP	This paper	N/A
M3R-GFP	(Wei et al., 2021)	N/A
M3R LL-AA-GFP	This paper	N/A
DsRed	Clontech Laboratories	632466
VSVG-GFP	Addgene	11912
VSVG DxE-AxA-GFP	This paper	N/A
VSVGct-GFP	(Li et al., 2017)	N/A
VSVGct LL-AA-GFP	This paper	N/A

(*Continued on next page*)

Continued

REAGENT or RESOURCE	SOURCE	IDENTIFIER
VSVGct DxE-AxA-GFP	This paper	N/A
VSVGct DxE-AxA/LL-AA-GFP	This paper	N/A
α_{2A}-AR-GFP	(Li et al., 2017)	N/A
α_{2A}-AR YS-AA-GFP	(Dong and Wu, 2006)	N/A
DsRed2-ER	(Dong and Wu, 2006)	N/A
Software and algorithms		
ImageJ	NIH	imagej.nih.gov/ij/

RESOURCE AVAILABILITY

Lead contact

Further information and requests for resources and reagents should be directed to and will be fulfilled by the Lead Contact: Guangyu Wu (guwu@augusta.edu).

Materials availability

Reagents generated in this study are available from the lead contact upon request.

Data and code availability

- All data reported in this paper will be available from the lead contact upon request.
- This paper does not report original code.
- Any additional information reported in this paper will be shared by the lead contact upon request.

EXPERIMENTAL MODELS AND SUBJECT DETAILS

Cell culture

HEK293 cells were cultured in Dulbecco's modified Eagle's medium (DMEM) with 10% fetal bovine serum (FBS), 100 units/ml penicillin and 100 μg/ml streptomycin. SHSY5Y cells were cultured in F12/Minimum essential medium (MEM) (V/V =1:1) with 10% FBS.

Preparation of primary neurons

Primary cultures of hippocampal neurons were prepared from embryonic day 18 Sprague-Dawley rat pups and grown on glass coverslips pre-coated with poly-L-lysine in Neurobasal medium supplemented with B27 and L-glutamine as described previously (Wei et al., 2021). The preparation of primary neurons from timed-pregnant rats was approved by the Augusta University Institutional Animal Care & Use Committee (IACUC).

Animals

Pregnant female Sprague-Dawley rats (E14), aged 8-10 weeks, were purchased from Charles River for the isolation of primary hippocampal neurons. The use and care of animals used in this study follows the guidelines of the Augusta University IACUC.

METHOD DETAILS

Plasmid constructions

α_{2B}-AR, α_{2A}-AR, β_2-AR and M3R tagged with GFP at their CT were generated as described previously (Dong et al., 2010b; Filipeanu et al., 2006; Wei et al., 2021). The chimeric constructs β_2ARα_{2B}ct in which the CT of β_2-AR was substituted with the CT of α_{2B}-AR and VSVGct in which the C-terminal helical region of AT1R was fused to the CT of VSVG were generated as described previously (Dong et al., 2010a; Li et al., 2017). The mutants of receptors and VSVG were generated by QuikChange site-directed mutagenesis, using primers (Table S1). All constructs used in the present study were verified by nucleotide sequence analysis.

Transient transfection

To visualize receptor expression at the dendritic and post-synaptic compartments by confocal microscopy, hippocampal neurons were transfected using Lipofectamine 2000 reagent (Thermo Fisher Scientific) as described previously (Wei et al., 2021). Transient transfection of cells was carried out by using Lipofectamine 2000 as described previously (Wu et al., 2003).

Fluorescence microscopy

For image acquisition and quantification of receptor expression at the dendritic and post-synaptic compartments, hippocampal neurons were fixed with 4% paraformaldehyde and 4% sucrose for 15 min and washed with phosphate-buffered saline (PBS) for 3 times. Images were captured with a ×40 objective on a Zeiss LSM780 confocal microscope. Confocal images were analyzed and quantified with the ImageJ software (NIH). Dendritic receptor expression was measured as the dendritic area expressing individual receptors. To measure receptor expression at post-synapses, spines of secondary dendrites and adjacent dendrite shaft regions were defined under the DsRed channel and post-synaptic receptor expression was measured by the ratio of spine over dendritic shaft expression as described previously (Wei et al., 2021).

For analysis of receptor localization in HEK293 and SHSY5Y cells, the cells were grown on coverslips precoated with poly-L-lysine on 6-well dishes and transfected with 500 ng of receptor for 36-48 h. To study receptor colocalization with the ER, the receptors were co-transfected together with DsRed-ER. To study receptor expression at the Golgi, the cells were fixed and permeabilized with PBS containing 0.2% Triton X-100 for 5 min. After blocking with 5% normal donkey serum for 1 h, the cells were sequentially stained with primary antibodies against GM130 or giantin (1:200 dilution) for 1 h and fluorophore-conjugated secondary antibodies (1:2000 dilution) for 1 h. Images were captured with a ×63 objective on Zeiss LSM780 or Leica Stellaris 5 confocal microscopes as described previously (Wei et al., 2019).

Radioligand binding of intact live cells

Intact cell radioliagnd binding to measure α_2-AR, β_2-AR and M3R was carried out by using [^{3}H]-RX821002,[^{3}H]-CGP12177 and [^{3}H]-NMS, respectively, as described previously (Li et al., 2012; Wei et al., 2021). In brief, individual receptors and their mutants were transiently expressed and the cells were then incubated with respective radioligands at 20 nM for 90 min at room temperature. The cells were washed twice with 1 ml of PBS, and then treated with 500 μl of 1M NaOH for 1 h. The radioactivity was counted by liquid scintillation spectrometry in 4 ml of Ecoscint A scintillation solution. Non-specific binding of α_2-AR, β_2-AR and M3R was determined in the presence of rauwalscine, alprenolol and atropine at 20 μM, respectively.

Measurement of VSVG transport from the ER to the Golgi

The transport of VSVG was measured by using its temperature sensitive mutant (VSVGtsO45) which was misfolded and retained within the ER at the restrictive temperature 40°C and correctly delivered to the Golgi at the permissive temperature 32°C (Presley et al., 1997). Cells grown on coverslips in 12-well dishes were transfected with 0.25 μg of VSVGtsO45-GFP or its mutants. The cells were cultured for 24 h at 40°C to induce the accumulation of VSVG in the ER and then transferred to 32°C for 30 min to allow VSVG to transport to the Golgi. After fixation, the subcellular localization of VSVG was visualized by confocal microscopy. The cells with VSVG expression at the Golgi were counted, and at least 40 cells were counted in each experiment as described previously (Li et al., 2017).

QUANTIFICATION AND STATISTICAL ANALYSIS

Details regarding the quantification of receptor and VSVG expression in primary neurons and/or cell lines are provided in the method details section. All data were calculated and presented as mean ± SE. Statistical analysis was performed using unpaired Student's t test or one-way ANOVA test. $p<0.05$ was considered as statistically significant.